



Detection of Water and Ice on Bridge Structures by AC Impedance and Dielectric Relaxation Spectroscopy, Phases III and IV: Continued Field Testing and Refinement of Novel Water and Ice Sensor Systems on Bridge Decks

Final Report

Prepared by:

John F. Evans

Department of Chemistry and Biochemistry
University of Minnesota Duluth

Northland Advanced Transportation Systems Research Laboratories (NATSRL)
University of Minnesota Duluth

CTS 13-26

Technical Report Documentation Page

1. Report No. CTS 13-26	2.	3. Recipients Accession No.	
4. Title and Subtitle Detection of Water and Ice on Bridge Structures by AC Impedance and Dielectric Relaxation Spectroscopy. Phaseu III and IV: Continued Field Testing and Refinement of Novel Water and Ice Sensor Systems on Bridge Decks		5. Report Date August 2013	
		6.	
7. Author(s) John F. Evans		8. Performing Organization Report No.	
9. Performing Organization Name and Address Department of Chemistry and Biochemistry University of Minnesota Duluth 1039 University Drive Duluth, Minnesota 55812		10. Project/Task/Work Unit No. CTS # 2011011 and 2012017	
		11. Contract (C) or Grant (G) No.	
12. Sponsoring Organization Name and Address Intelligent Transportation Systems Institute Center for Transportation Studies University of Minnesota 511 Washington Avenue SE, Suite 200 Minneapolis, Minnesota 55455		13. Type of Report and Period Covered Final Report 7/1/10 – 8/31/12	
		14. Sponsoring Agency Code	
15. Supplementary Notes http://www.its.umn.edu/Publications/ResearchReports/			
16. Abstract (Limit: 200 words) During Phases III and IV of this project it was determined that the physical attributes of the prototypes developed during the earlier work was inappropriate for bridge deck installations. Mn/DOT engineers required that they be planar and not require drainage through the deck. As RWIS platforms had been widely deployed on decks throughout the state, we decided to adhere to the RWIS geometric format. This necessitated a significant re-engineering of the sensor hardware before installation and testing at remote bridge sites could proceed. To that end extensive development of a robust sensor meeting these requirements was developed and tested without compromise to the earlier performance results. In large part the maintenance of performance was achieved through a significant modification of the software to include Wavelet analysis of the raw data in the determination of surface state of the sensor platform (ice vs air vs water vs electrolyte present on the sensing electrode structure). The combined regression results for raw TDR responses treated by three analysis procedures are shown to give rise to very reliable results. Unfortunately, remote field testing of sensors installed on bridge decks was not accomplished.			
17. Document Analysis/Descriptors Snow and ice control, Sensors, Ice sensing, Snow sensing, Weather sensors, Safety		18. Availability Statement No restrictions. Document available from: National Technical Information Services, Alexandria, Virginia 22312	
19. Security Class (this report) Unclassified	20. Security Class (this page) Unclassified	21. No. of Pages 32	22. Price

Detection of Water and Ice on Bridge Structures by AC Impedance and Dielectric Relaxation Spectroscopy, Phases III and IV: Continued Field Testing and Refinement of Novel Water and Ice Sensor Systems on Bridge Decks

Final Report

Prepared by:

John F. Evans

Department of Chemistry and Biochemistry
University of Minnesota Duluth

Northland Advanced Transportation Systems Research Laboratories (NATSRL)
University of Minnesota Duluth

August 2013

Published by:

Intelligent Transportation Systems Institute
Center for Transportation Studies
University of Minnesota
511 Washington Avenue SE, Suite 200
Minneapolis, Minnesota 55455

The contents of this report reflect the views of the authors, who are responsible for the facts and the accuracy of the information presented herein. This document is disseminated under the sponsorship of the Department of Transportation University Transportation Centers Program, in the interest of information exchange. The U.S. Government assumes no liability for the contents or use thereof. This report does not necessarily reflect the official views or policies of the Northland Advanced Transportation Systems Research Laboratories, the Intelligent Transportation Systems Institute or the University of Minnesota.

The authors, the Northland Advanced Transportation Systems Research Laboratories, the Intelligent Transportation Systems Institute, the University of Minnesota and the U.S. Government do not endorse products or manufacturers. Trade or manufacturers' names appear herein solely because they are considered essential to this report.

Acknowledgements

The author(s) wish to acknowledge those who made this research possible. The study was funded by the Intelligent Transportation Systems (ITS) Institute, a program of the University of Minnesota's Center for Transportation Studies (CTS). Financial support was provided by the United States Department of Transportation's Research and Innovative Technologies Administration (RITA).

The project was also supported by the Northland Advanced Transportation Systems Research Laboratories (NATSRL), a cooperative research program of the Minnesota Department of Transportation, the ITS Institute, and the University of Minnesota Duluth College of Science and Engineering.

The assistance of Mr. Evan Anderson and Mr. Luke Busta in the execution of this research project is gratefully acknowledged.

Table of Contents

Chapter 1: Task Specifications	1
Chapter 2: Introduction	3
Chapter 3: Technical Background.....	5
Chapter 4: Refinement of Sensor Design.....	9
Chapter 5: Refinement of Data Processing Software	13
Chapter 6: Exploration of Signal Processing Hardware Alternatives.....	19
Chapter 7: System Deployment and Field Testing	21
References.....	23

List of Figures

Figure 3.1 Voltage vs time at a point on an impedance mismatched transmission line driven with a step voltage of height E_i	6
Figure 3.2 Transmission line with 6 dielectric discontinuities	6
Figure 3.3 Idealized TDR trace for a series RC terminated transmission line	7
Figure 4.1 RWIS (Lufft model IRS21) sensor package showing various sensing devices	9
Figure 4.2 Final ruggedized-sensor platform, including field-replaceable passive sensor. Thermistor (backside contact to aluminum plate) connections are not shown.	10
Figure 4.3 Photograph of final design of the sensor platform with replaceable sensor mount (white rectangle) removed from the overall system and placed to its left. This design allows for the sensor to be field replaceable in the event of mechanical or electrical failure, or when sensor designs with improved response are developed.....	10
Figure 4.4 Long term performance of final sensor design (Fig. 4.2). Each grouping shows FOM values left to right corresponding to 0, 7, 14, 35, 42, 49 and 54 days after the initiation of the study. See following chapter for definition of the FOM value	11
Figure 5.1 Overall signal processing scheme yielding a single real-time figure of merit (FOM) for sensor response correlated against bank of standards	14
Figure 5.2 Example Freeze-thaw cycle for water from “remote” sensor located in the test stand. Raw data acquired by the datalogger transmitted to a “central” processing station running in-house developed software (written in LabVIEW).	14
Figure 5.3 Example of results from final sensor prototype (Fig. 4.2) showing oscillations of FOM values during a thaw-evaporation cycle. The traces are identified as water FOM – red, ice FOM – blue, and air FOM – green and centigrade temperature purple. The sensor is in contact with frozen water at time 0, after which it undergoes a thaw to liquid water (~100 min) and finally evaporation of the water (300-600 min) to leave the sensor surface in contact with air as the temperature rises from -6 C initially to room temperature (18 C) after 300 min	15
Figure 5.4 Flow chart of finalized data analysis software employed to provide real time output of surface conditions reported as dry, wet or icy from a given sensor. Note all calculations are carried out after remote data has been sent via wireless modem to the central processing station where all standard responses and tracking histories are stored.....	16
Figure 5.5 LabVIEW Virtual Instrument front panel for overall system.	17
Figure 5.6 State output for thawing/evaporation cycle for an ice covered sensor (Fig. 4.2) as evaluated by consideration of highest FOM only (red trace) compared to more sophisticated analysis taking into account the thermal and state history for the cycle (black trace).....	18

Executive Summary

A low-cost system has been developed and tested that can accurately determine the surface condition of bridge decks with respect to whether or not safe conditions are present. The technology is based on the use of time domain reflectometry as applied to arrays of passive sensors from which raw data is acquired remotely and then forwarded to a central processing station where software compares the raw sensor data to a library of calibration data for each sensor. A simple output result (dry, wet, ice) regarding surface state of each sensor is provided, which can then be employed to activate traffic signage at the remote site and/or notify maintenance personnel as to the need for the application of deicing chemicals.

Chapter 1

Task Specifications

This report covers FY 2011 and FY 2012. As such, the tasks listed in the original proposals are listed below, and will be cross referenced in the following chapters which describe the evolution of sensor, system and software development.

FY 2011

1. Sensor Redesign per MnDOT Requirements for Deployment: This task will involve a final redesign of our prototype sensor to meet installation requirements of the D-1 MnDOT engineers, so that they may be installed in a bridge deck in Task 2. *See Chapter 4-5*
2. Installation of Sensors and TDR System with Remote Power and Connectivity: This task will involve working with MnDOT personnel to deploy a system of eight multiplexed sensors and the complete TDR system to a bridge deck near Duluth, MN. *See Chapter 7*
3. Installation of Sensors and TDR System: This task will involve deployment of a system of two multiplexed sensors and the complete TDR system at the NATSRL Cloquet test facility near Duluth, MN. *See Chapter 7*
4. Evaluation of Remote System performance over the Winter Season 2010-11: This task will involve continual evaluation of system performance relative to weather and road surface conditions for the coming winter season. *See Chapter 7*
5. Draft and Final Report Completion: A draft final report will be prepared following the ITS publication guidelines to document project activities, findings and recommendations. This report will be submitted through the publication process for technical and editorial review. A revised final report incorporating the review comments will be prepared and submitted for publication. *This Document*

FY 2012

1. Continued Sensor and System Design Enhancements per MnDOT Requirements for Deployment: This task will involve continued improvements in the sensor to meet installation requirements of the D-1 MnDOT engineers. *See Chapters 4-6*
2. Expansion of D-1 Bridge Install to Include Multiple, Redundant Sensors and TDR System with Remote Power and Connectivity: This task will involve working with MnDOT personnel to deploy a system of *eight multiplexed sensors* and the complete TDR system to a bridge deck near Duluth, MN. *See Chapters 7*
3. Evaluation of Remote System performance over the Winter Season 2011-12: This task will involve continual evaluation of two deployed system performance relative to weather and road surface conditions for the coming winter season. One will be at the Cloquet Lab and the second (Task 3) at a D-1 Bridge Site. *See Chapters 7*
4. Draft and Final Report Completion: A draft final report will be prepared following the ITS publication guidelines to document project activities, findings and recommendations. This report will be submitted through the publication process for technical and editorial review. A revised final report incorporating the review comments will be prepared and submitted for publication. *This Document*

Chapter 2 Introduction

Our research objective, simply stated, has been to develop reliable, low-cost water/ice sensors systems which can be deployed in a variety of critical locations. Our aim is to develop these technologies in configurations amenable to inclusion in remote sensing networks.

In light of the lack of affordable alternative ice/water detection systems, if we are successful, these outcomes could provide revolutionary sensing alternatives to those currently available. The benefits could be enormous in terms of decreasing loss of life, personal injury and loss of property at critical sites by virtue of making real time data available to trigger automated dispensing systems, or alert maintenance crews of immediate need for application of deicing chemicals to these critical areas. The primary benefits would accrue to the public in terms of reduced accident risk at critical traffic sites.

During Phases I and II of this project, we have carried out the evaluation of a novel approach to low-cost sensing system for monitoring ice, water and deicing solutions on road bridge deck surfaces. The technology is based on the use of passive sensors which terminate a transmission line. Time domain reflectometry (TDR) is employed to capture reflected pulse waveforms from the sensor which are found to provide transient responses which are unique not only to a particular sensor design, but also the dielectric properties of the medium in contact with the sensor. In that the dielectric properties of the media to be sensed (e.g. air, water, ice, electrolyte and frozen electrolyte) give rise to different responses, these can be used to determine the local conditions at the sensor.

Phase II explored various aspects of sensor design, and empirically determined design guidelines were determined. First generation software was written in LabVIEW to process data acquire from the sensors to establish the state of precipitation or deicing solutions in contact with them. Commercial electronics were specified and a system with remote data gathering supported by a central processing station was assembled and tested.

Although these results were very encouraging, the project required further refinement of sensor and software design, as well as actual field testing of a system. To that end the following guidelines were established for the final hardware (sensor) and software (signal processing) improvements prior for systems to be deployed on a bridge deck for actual field testing:

1. Refinement of sensor design to optimize performance (air vs ice differentiation) and provide a mechanically robust configuration which is in a package amenable for installation in a bridge deck (as approved by MnDOT bridge engineers).
2. Refinement of data processing software to enhance differentiation between different media (including liquid and frozen electrolyte solutions to mimic deicing chemicals).
3. Actual deployment of a system onto a bridge deck after these refinements have been made for real world testing of a system.

Chapter 3

Technical Background

Time Domain Reflectometry. Time domain reflectometry (TDR) is a technique used to test electrical interconnects and transmission lines in high speed circuitry (e.g. serial disk drive communication protocols, Ethernet cabling systems, etc.). Any changes in the impedance of the current path (transmission line) can be mapped, because these cause reflections at the interfaces between domains of differing impedance (as indicators of differences in dielectric constant of the medium surrounding the transmission line). The technique relies on variation in the dielectric relaxation of media in contact with the transmission line, and, furthermore, the location of discontinuities in the dielectric properties of the adjacent media can be determined. As such, simple sensing systems, which are directly amenable to remote sensing situations, can be realized. This approach has been applied to a wide range of systems, although the primary application has been to soil samples, and evaluation of volumetric water content in these samples. It should be noted that frozen water in soils and electrolyte salt concentration in soils have been measured, as well. Furthermore, the sensors themselves (elements of a transmission line) are very inexpensive. Examples of recent applications of this technology to sensing (as opposed to testing) include measurement of resin flow in polymer curing applications¹, water and ice content in soil systems^{2,3,4}, and detection of ice, water and deicing solutions of aircraft wings and rotors.⁵ Indeed because of the ease with which dielectric relaxation measurements can be made over such a wide frequency range (1 MHz to 20 GHz), TDR has been applied to fundamental research involving the structure of water⁶ and the relaxation of water bound to silica gel.⁷

Like impedance spectroscopy, TDR allows one to measure dielectric relaxation, but at a much higher frequency and bandwidth. Furthermore, in principle, changes in the complex dielectric function of material near the sensing transmission line elements can be resolved in terms of the positional dependence along the length of the transmission line to a resolution of a centimeter or less.

The effective real part of the dielectric “constant” of water is approximately 80, while that of ice is 3. The TDR technique can also be employed to measure the conductivity of salt solutions, such as the deicing systems commonly in use.

The detailed physics of TDR measurements cannot be presented in the framework of this report, so only a brief introduction will be given. The technique involves applying a very fast rise time (ps time frame) voltage pulse to one end of a transmission line. The pulse travels down the transmission line at a velocity nearing the speed of light, which depends on the dielectric properties of the medium surrounding the transmission line, according to:

$$v = c / \sqrt{\epsilon} = c / n$$

where, c is the velocity of light in vacuum, ϵ is the dielectric constant of the medium surrounding the transmission line and n is the complex refractive index of that medium.

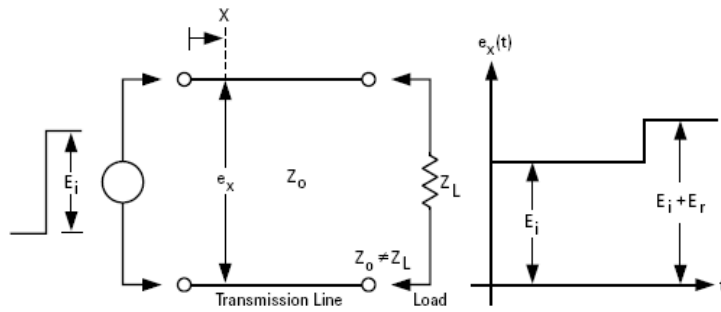


Figure 3.1. Voltage vs time at a point on an impedance mismatched transmission line driven with a step voltage of height E_i .

As depicted above, any point along or at the terminus of a transmission line where the impedance changes, due to a change in dielectric constant of the surrounding medium, a portion of the energy in the pulse is reflected back to the source. That portion of energy not reflected or adsorbed at a discontinuity continues down the line until it is either absorbed or reflected. The physical position of the discontinuity can be determined with appropriate calibration. For example, consider a segmented system as shown in the following figure:



Figure 3.2. Transmission line with 6 dielectric discontinuities.

As the launched pulse encounters each dielectric discontinuity (points 1-6), a portion of the energy is reflected back to the source. In addition to determining the location of these dielectric discontinuities, a more detailed analysis of the differential complex impedance of that reflection can be made, and from this analysis the effective dielectric constant determined and attributed to materials for which the dielectric properties have been previously calibrated (e.g. water, ice, and electrolyte solutions).

Figure 3.3 shows the reflected pulse for a terminal sensing arrangement in which R and C represent the circuit equivalence impedances associated with the conductivity and dielectric loss associated with a salt solution. Here the solution properties of the electrolyte (real part of the dielectric constant and conductance) may be extracted for the measured values of R and C .

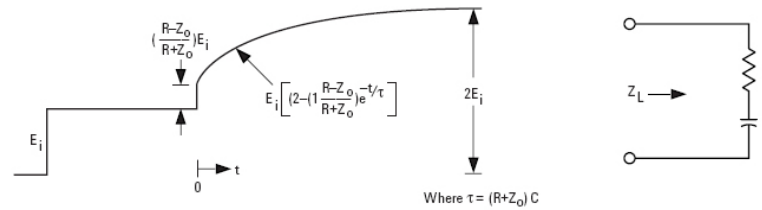


Figure 3.3. Idealized TDR trace for a series RC terminated transmission line.

Due to the significant difference in the real and imaginary components of the impedance of ice, water and deicing solutions, these boundaries are easily discerned.⁵ With respect to the spatial sensitivity and other design issues, reasonable care must be exercised in the physical and electrical design of the transmission line. Care must also be taken to impedance match the line to the source impedance of the TDR pulse generator, to preserve optimal sensitivity and spatial resolution. Given that transmission line theory is well established, such optimizations should be relatively straightforward. During the first year of this study the primary focus of the experimental work will be on the design of transmission lines in terms of geometry and materials employed, with consideration of segmented or continuous lengths of transmission lines also under consideration.

By analogy to the reported sensitivity to location and state of water on aircraft airfoil and airframe surfaces, we propose to examine the use of TDR to examine the state of water on various pavement and overlay surfaces.⁵ As in the case of the lower frequency impedance measurements, various fixtures will be examined to evaluate optimal geometry and placement of the sensor (transmission) line relative to the surface under test. The effectiveness and tradeoffs of long runs of transmission line sensor (TLS) will also be examined, to ascertain whether or not arrays and networks can be used to map the state of water across large areas of roadbed or bridge deck surface. In principle a single TLS should be useful over a 150 m distance, so long as the dielectric in contact with it is not overly lossy, permitting spatial resolution of approximately 1 cm. One of the most promising aspects of this technology is the ability to sample various segments of a single transmission line, multiple transmission lines or a combination of both using a single set of TDR electronics in conjunction with commercially available network switches. As such, it is possible that commercially available TDR systems used for soil water analysis in agricultural applications (e.g. Trace system with a model 6020 multiplexer from Soilmoisture Equipment Corp., Santa Barbara, CA) could provide the electronics package for a 256 TLS array system covering an entire bridge, at a cost of approximately \$20K. Not only would this provide a significant advantage over light based technologies which sample a single spot, but at a considerably lower cost per sensor site (\$20K/256 = \$78/sensor). Furthermore, many of these lower cost systems are configurable for remote sensing applications (wireless modems, Bluetooth modules and battery powered electronics) which are particularly attractive attributes for this application.

Chapter 4

Refinement of Sensor Design

During Phase II of this project⁸ we have demonstrated the proof on concept of the use of passive metal sensors and the TDR approach as applied to sensing bridge/road conditions. Many different geometries were explored, some of which were planar, while others were three dimensional. Some of the planar designs could be refined and ruggedized for practical deployment at a bridge deck site in a relatively straightforward manner, while the latter geometries, although more promising with respect to statistical differentiation of the medium in contact with the sensor (ice vs water, etc.). The basis for these comparisons is the correlation coefficient derived from simple regression of sensor response to standard responses for a given sensor exposed to ice vs air vs water⁹.

Early discussions with MnDOT bridge engineers led us to believe that non-planar sensor designs could be accommodated during installation by inserting these into a shallow hole afforded by coring into the deck, including a drain hole of smaller diameter through the bridge deck. As the project proceeded, it became apparent that such an approach to sensor installation was not acceptable, due to concerns about weakening the local deck structure around these holes. This forced a reconsideration of the tradeoffs between the sensor performance reflected by the correlation coefficients alluded to above and the overarching requirement of a planar design. As such, the following constraints for further sensor refinement were imposed. Firstly, the size and installation of the sensors under development here must be constrained by the MnDOT Road Weather Information System (RWIS) sensors already installed on many road and bridge surfaces in Minnesota and other locations world-wide.¹⁰ As such it can easily be inferred that if the structural intrusions required for RWIS sensor system installations are tolerable, then the sensors under development here would also be acceptable.. Secondly, all practical sensors developed here must be generally planar, and not require any special drainage considerations (e.g. drainage holes drilled through the deck). This second constraint is again consistent with the RWIS package.

For clarity, the RWIS sensor systems (IRS21 Lufft Intelligent Road Surface Sensor marketed in the US by Campbell Scientific, Logan, UT) is briefly discussed here as its design relates to the constraints outlined above. More detail can be found in the specifications of these systems.¹⁰ Shown in Figure 4.1, below, is the RWIS sensor.



Figure 4.1 RWIS (Lufft model IRS21) sensor package showing various sensing devices.

The system platform shown above is specified to be 5 inches in diameter and 2 inches high. The typical installation is made into a 3 inch deep, 6 inch diameter bore hole as described in the installation manual.¹⁰

After attaching the requisite cabling, the device is level set with the deck surface, and both it and the cabling (laid in a ½ inch wide saw cut) are potted in fast setting epoxy.

To accommodate a similar installation approach a planar platform for our sensors was designed and constructed. Included in this design was a provision for the replacement of the sensor (mounted on a 2 x 4.5 x 0.5 in polypropylene sheet) without removal of the platform from an installation site. Temperature measurement using a thermistor was also included. Shown in Figure 4.2 is the assembled platform. The additional threaded holes are to accommodate the leveling of the device during installation. In this case the sensor is comprised of parallel 0.188 in thick rectangular stainless steel electrodes separated by a 0.125 in thick silicone rubber spacer. The overall diameter of the aluminum platform is 5.0 in and the thickness is 1.25 in, consistent with the RWIS platform dimensions.

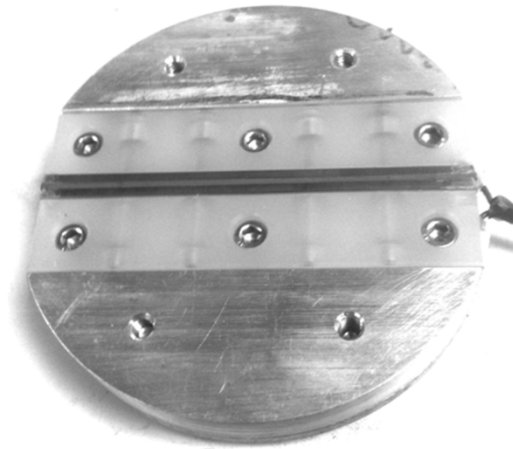


Figure 4.2 Final ruggedized-sensor platform, including field-replaceable passive sensor. Thermistor (backside contact to aluminum plate) connections are not shown.

The modularity of this platform is shown in Figure 4.3 where the blank sensor panel is shown on the left with the platform and sensor cable connector on the right.



Figure 4.3 Photograph of final design of the sensor platform with replaceable sensor mount (white rectangle) removed from the overall system and placed to its left. This design allows for the sensor to be field replaceable in the event of mechanical or electrical failure, or when sensor designs with improved response are developed.

Electrical connections between the sensor and the TDR electronics were made with RG-174 coaxial cable to ensure the preservation of the signal integrity of excitation and reflected waveforms, and to match impedance output of the TDR system. Electrical connections to the thermistor mounted to the back side of the platform are not shown here. Although other electrode and dielectric materials and dimensions were investigated, most measurements were made with this configuration.

The long term reliability performance of the final prototype (see Figure 4.2) was evaluated over an extended period of time (54 days) under laboratory conditions (temperature-controlled environmental test chamber). Using the final signal processing scheme described in the next chapter, in which sensor performance is given by a figure of merit (FOM) value ranging from 0 to 3 for these data, and focusing on the surface media conditions which are most challenge to differentiate (ice vs air) due to their similar dielectric constants (4 vs 0, respectively), the results are summarized in Figure 4.4. Within each regression of sample medium compared to standard medium we note nearly perfect correlation ($FOM > 2.95$) when sample and standard are the same, and consistently low ($FOM < 1.5$) when an ice sample is compared to and air standard or vice versa.

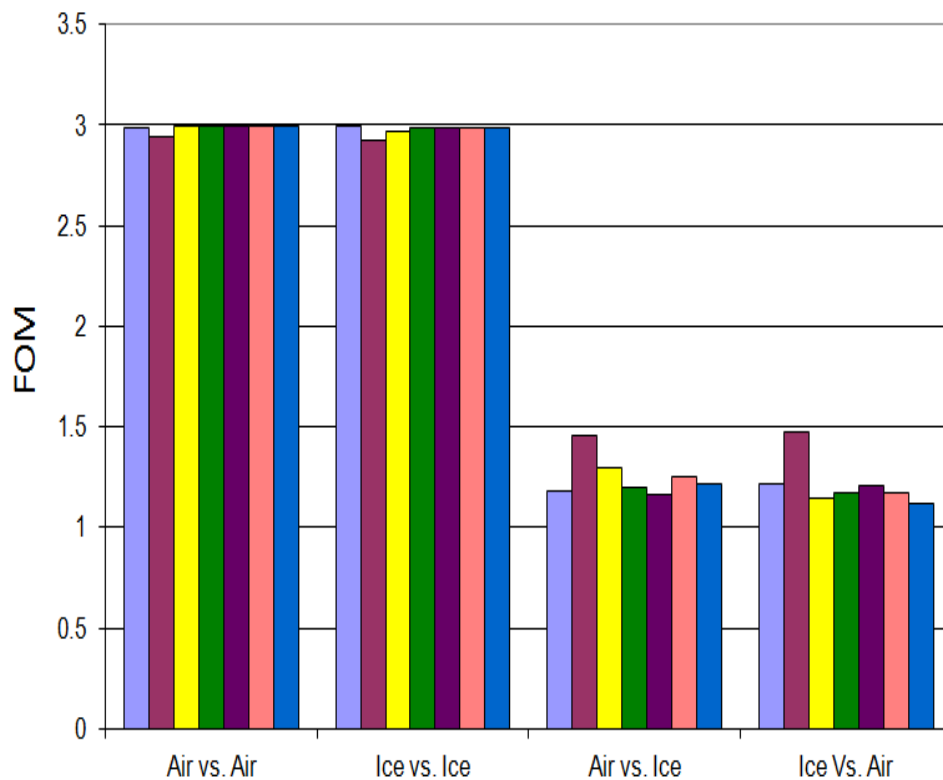


Figure 4.4. Long term performance of final sensor design (Figure 4.2). Each grouping shows FOM values left to right corresponding to 0, 7, 14, 35, 42, 49 and 54 days after the initiation of the study. See following chapter for definition of the FOM value.

Chapter 5

Refinement of Data Processing Software

The constraints of a rugged, planar sensor platform as discussed in the previous chapter required the development of a more sophisticated data analysis approach to ensure optimal performance in identification of surface conditions detected by these systems. As discussed in the Phase II Final Report, the data acquisition parameters had been optimized⁹, and these remained constant during the current phase. During Phase II in which the primary focus was the exploration of sensor design, geometry and materials of construction, relatively simple data analysis software was employed.⁹ Briefly, the raw TDR transient waveforms were differentiated, followed by digital filtering employing a 21 point, 3rd order polynomial. Temperature corrections and adjustments for slight variation in the length of the connecting cables was then applied using a straight forward time shift based on the early response peak in the derivative signal. The sensor waveform under test was then correlated against known standard responses (previously determined under known conditions; i.e. exposure to air, ice, water, etc.) for that sensor. The correlation coefficient returned from this correlation (R^2_{der}) yielded values ranging between 0 (uncorrelated) to 1 (perfectly correlated). The most challenging differentiation for all prototype sensor designs was found to be between ice and air for the media in contact with the sensor electrodes.

To improve upon the ability of a sensor to identify the medium in contact with its electrodes, a more sophisticated data analysis approach was taken. This included the addition of analysis of frequency content of the differentiated/smoothed TDR waveforms for both standard and unknown media responses for a given sensor. Typically Fourier analysis is used for this purpose.¹¹ An improved approach employing the wavelet transform¹² which uses more complex base functions called wavelets was used, as opposed to the sine-cosine functions in the case of the Fourier transform. The use of a “mother” wavelet which is scaled in time has been shown to provide more robust frequency analysis without the frequency resolution issues that accompany Fourier analysis.¹³ While the wavelet transform has been most widely applied to image processing^{14,15} and comparisons between this approach and Fourier-based methods have been drawn¹⁶, our use for this project is relatively simple. To obtain a relatively global indication of high and low frequency content of the smoothed derivative TDR waveforms reported by a sensor, we use wavelet transformations to obtain a snapshot of the low and high frequency content of these via a multiscale analysis (trending analysis). As such each smoothed derivative TDR waveform (sample as well as standards) is subjected to such analysis as implemented in LabVIEW and the results of sample results compared to a bank of standards of known contact media (ice, water, air, etc.). The low and high frequency content for a sample waveform is then correlated with its standard counterpart to give two additional regression coefficients R^2_{hf} and R^2_{lf} for the high and low frequency components, respectively. Each of these ranges between 0 (uncorrelated) to 1 (perfectly correlated), similarly to R^2_{der} , are discussed above. Finally we add these three correlation coefficients together to obtain the figure of merit (FOM) for a given comparison of sample to standard for a calibrated sensor. This FOM ranges from 0 – 3 and is taken as the single indicator of best match between sample (unknown surface condition) to standard (previously calibrated response to a known surface condition). While rarely yielding a perfect FOM = 3, simple sensors of simple geometries such as that shown in Figure 4.2 can yield values approaching that (e.g. FOM > 2.9). Moreover, correlation with the “incorrect” standards often yields values of FOM < 1).

The overall approach is depicted in Figure 5.1 on the following page.

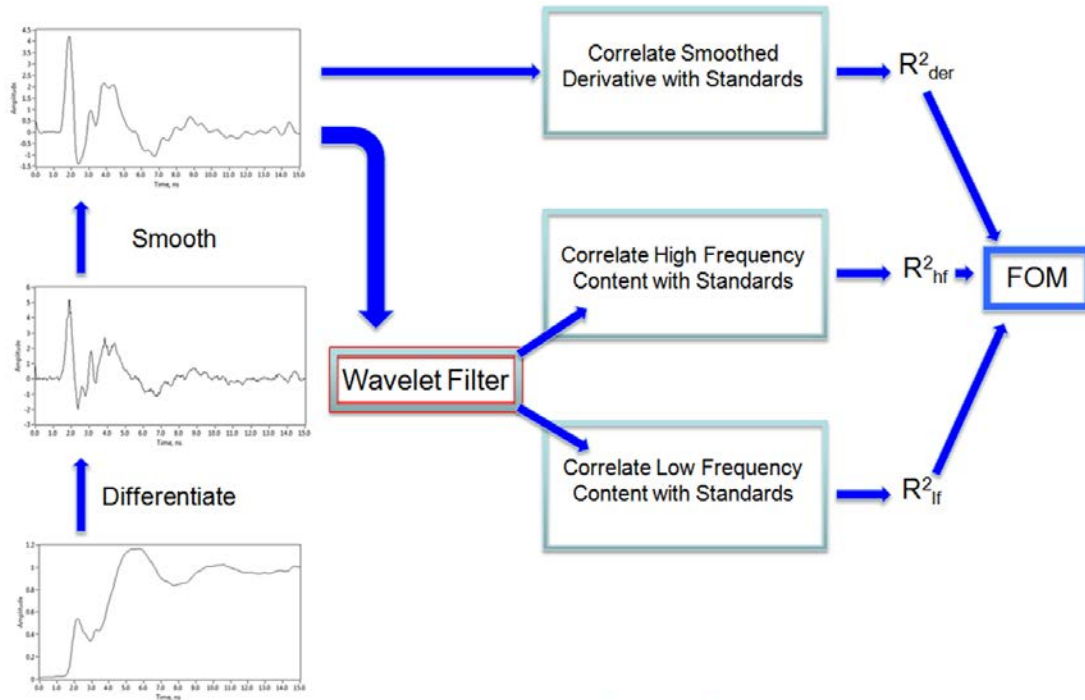


Figure 5.1 Overall signal processing scheme yielding a single real-time figure of merit (FOM) for sensor response correlated against bank of standards.

An example of this approach showing a freezing cycle for a sensor exemplified by that in Figure 4.2 is given below:

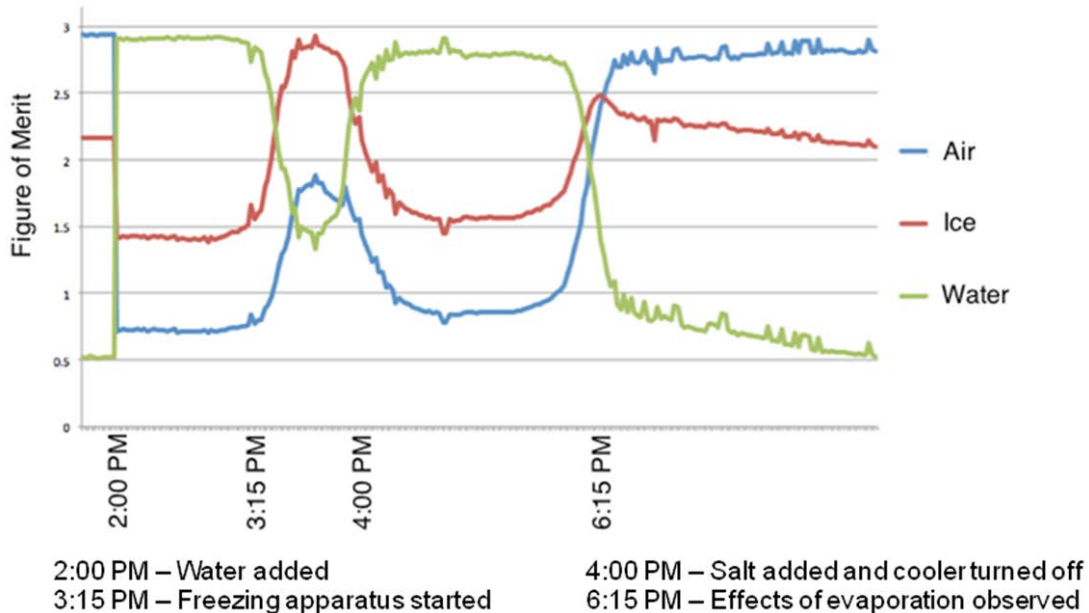


Figure 5.2 Example Freeze-thaw cycle for water from “remote” sensor located in the test stand. Raw data acquired by the datalogger transmitted to a “central” processing station running in-house developed software (written in LabVIEW).

The three curves are the results of correlations between the real time sample waveform (exposed first to air, then water, then ice, then salt solution and back to air) and the standard responses for this sensor which were previously obtained under controlled conditions. Each curve shows how the FOM varies for regression to air, water and ice standards. As such the lack of correlation (low FOM) for the regression to the ice standard *prior to freezing* compliments the high degree of correlation of the regression to the water standard during this period (2:00 – 3:15 pm). The utility of a single indicator of surface condition for each standard thus simplifies logical handling of these to yield a final safe vs dangerous condition which can be used to alert maintenance crews or drivers (via signage) to unsafe conditions.

While these results are very encouraging, the practicality of the entire approach relies on timely system responses regarding the bridge deck conditions (e.g. ice present on the surface) as the surface conditions change from, say from water to ice. These transition regions are somewhat more challenging in terms of defining the “safe” vs “unsafe” condition, for example the transition at 3:15 pm in the figure above. These transition regions must be treated with a more sophisticated approach, which requires data acquired and analyzed at a much higher real-time rate than depicted in Figure 5.2.

A more detailed data set for a thawing cycle is shown in the following figure:

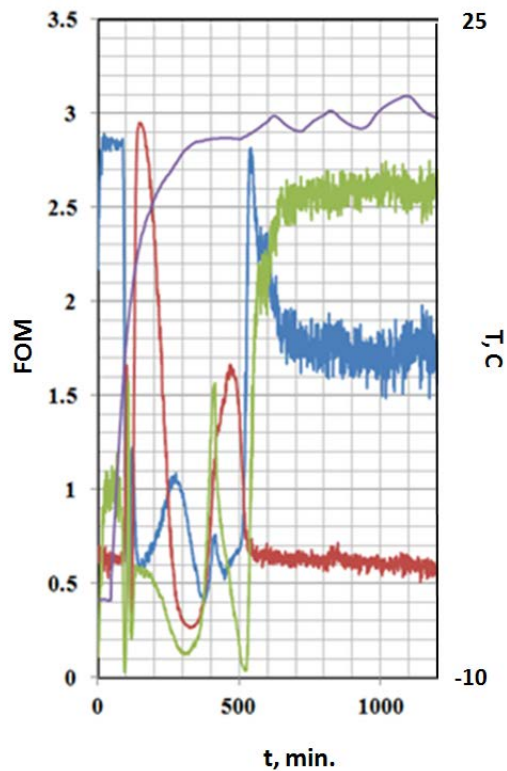


Figure 5.3 Example of results from final sensor prototype (Fig. 4.2) showing oscillations of FOM values during a thaw-evaporation cycle. The traces are identified as water FOM – red, ice FOM – blue, and air FOM – green and centigrade temperature purple. The sensor is in contact with frozen water at time 0, after which it undergoes a thaw to liquid water (~100 min) and finally evaporation of the water (300-600 min) to leave the sensor surface in contact with air as the temperature rises from -6 C initially to room temperature (18 C) after 300 min.

Here it is obvious that conclusions drawn only from an evaluation of the instantaneous FOM data are unreliable (see regions from 250 – 520 min). For example, using only the highest FOM value as the predictor of surface condition would suggest that the sensor was in contact with ice at $t = 280$ min., which is not the case. In fact at this point in time the sensor was partially covered in water and with the

remainder exposed to air. These issues were addressed in a further software revision, which took into account the sensor history (i.e. state definition prior to the current point in time) and the platform temperature. The states were categorized as wet, dry or icy, with the latter two including liquid and frozen electrolyte solutions (various concentrations of sodium and calcium chloride solutions intended to mimic typical solid deicing chemicals).

To remedy this lack of robust, reliable final result provided by the signal processing system, the program was elaborated to take into account the sensor history data (raw waveform and temperature) along with the standard responses in the form of two databases for each. The overall structure is outlined in Figure 5.4.

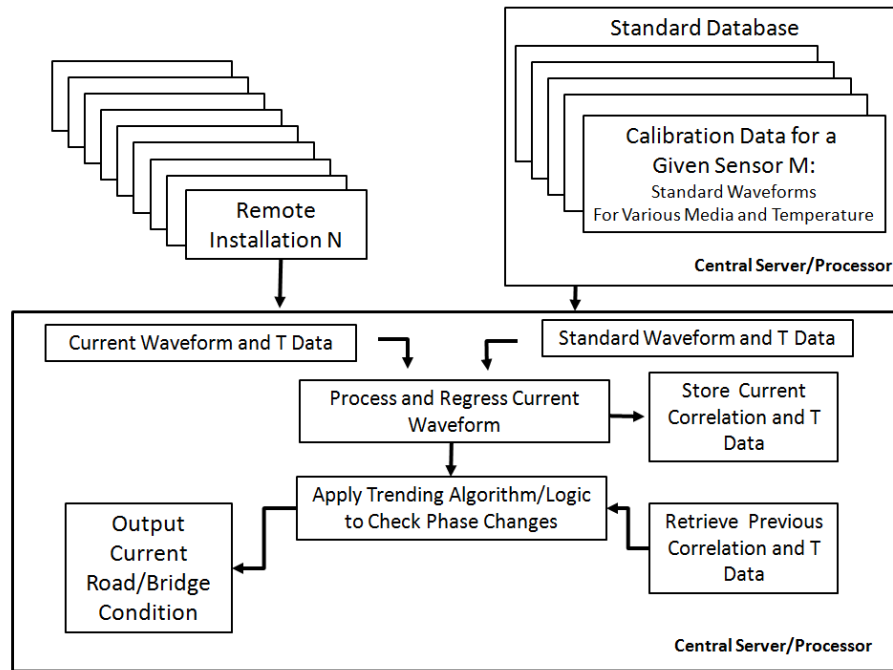


Figure 5.4 Flow chart of finalized data analysis software employed to provide real time output of surface conditions reported as dry, wet or icy from a given sensor. Note all calculations are carried out after remote data has been sent via wireless modem to the central processing station where all standard responses and tracking histories are stored.

Figure 5.5 shows the LabVIEW front panel of this software where it can be noted that real time monitoring of the sensor waveforms is accomplished both graphically, along with temperature standard responses and the current acquired sensor waveform. Most notably, the complex data processing and fitting results are distilled to a simple octal representation: the current surface state reported by the “LED” displays shown in the middle of the panel.

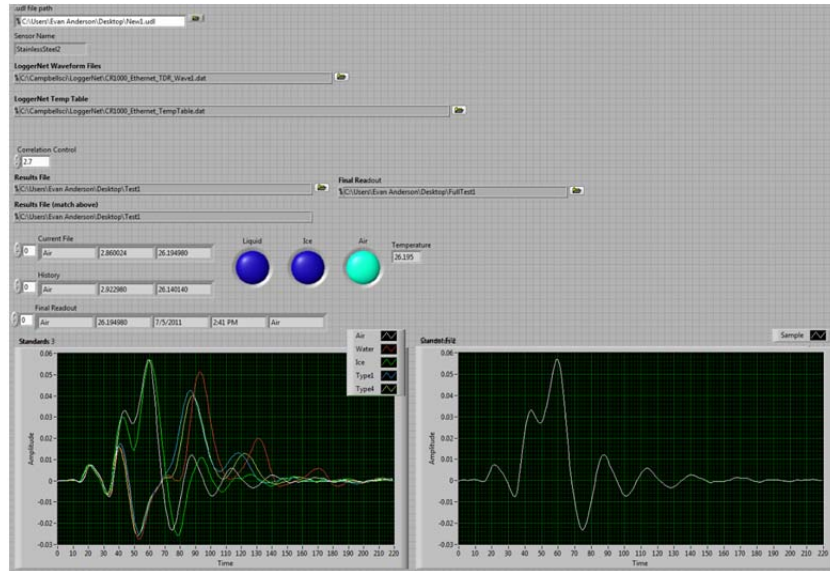


Figure 5.5. LabVIEW Virtual Instrument front panel for overall system.

This approach which included various logical/time dependent considerations included in the “Trending Algorithm/Logic” section shown above proved to provide completely accurate and robust output of the current sensor state during freezing and thawing cycles of water and various electrolyte solutions which approximated differing concentrations of salt-based deicing solutions typically applied from spreader plows. An example of the performance of this software enhancement compared to reliance on the FOM from regression to standard responses is shown in Figure 5.6.

This laboratory-based experiment involved the examination of a thawing/evaporation cycle for ice transitioning ultimately to air on a sensor identical to that shown in Figure 4.2. Data was acquired and analyzed every 30 s. Figure 5.6 depicts a comparison between the surface state determined by the FOM (red trace) alone vs that from the software enhancement described above (black trace). For the “surface state” output plotted on the ordinate, values of 3, 2 and 1 correspond to frozen water (ice), liquid water and dry (air), respectively, in contact with the sensor surface. The abscissa is the acquisition cycle, with a measurement taken every 30 s. The ice was visually observed to melt at cycle 162, 81 minutes into the run, and at 364 (182 minutes) the water had evaporated.

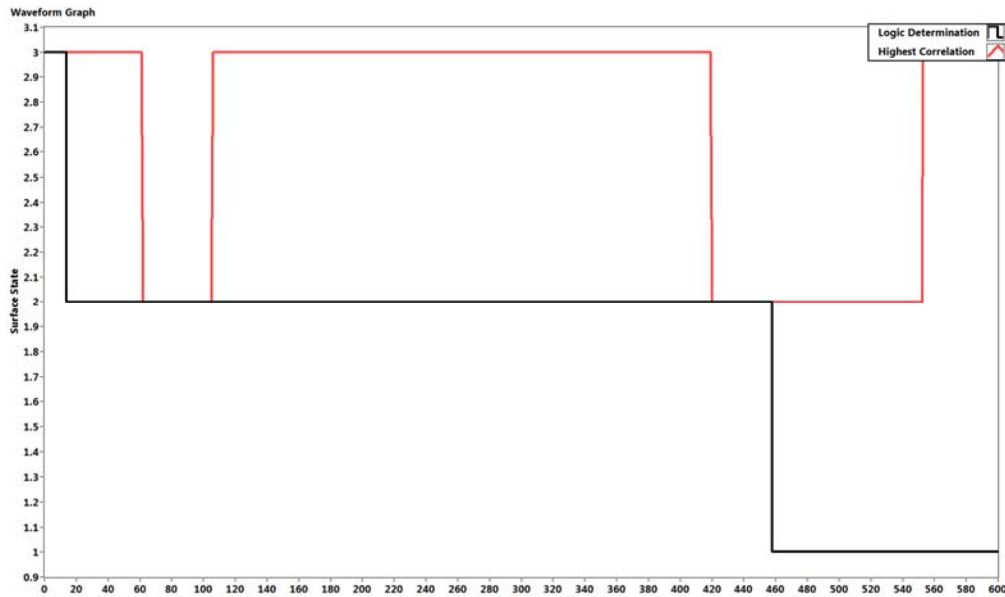


Figure 5.6. State output for thawing/evaporation cycle for an ice covered sensor (Figure 4.2) as evaluated by consideration of highest FOM only (red trace) compared to more sophisticated analysis taking into account the thermal and state history for the cycle (black trace).

Clearly the enhanced software is more robust in predicting surface state of the sensor in an accurate and timely fashion. Using FOM alone the indicated transitions are late, and in particular, where the state is most challenging to discern (air vs ice), the incorrect state is reported by the FOM alone. We conclude that this error is a direct result of the presence of both water and air in contact with different spots on the sensor. The enhanced software is not susceptible these errors. Similar results were obtained for both freezing and thawing experiments on this and other sensors for both water and electrolyte solutions up to 1.0 M in concentration (NaCl electrolyte).

Chapter 6

Exploration of Signal Processing Hardware Alternatives

Given the processing intensive requirements dictated by the enhanced software, and the expectation that an extended system with many installations and multiple sensors at each, we invested considerable effort in evaluating the possibility of local (site-based) processing of the TDR waveform results. As such, a significant portion of the real time computational load, could be offloaded from the central processing system supporting the entire distributed system.

In that we were heavily invested in software development in the LabVIEW environment, our evaluations were necessarily restricted to low-cost signal processing hardware options offered by National Instruments (NI). The primary requirements of this hardware including finding a vendor of TDR hardware which could bundled with such devices, and USB connectivity between TDR electronics and the signal processing hardware was paramount. A vendor of such a TDR system was located and we proceeded with evaluation of various economical single board or compact remote signal processing systems offered by NI (field point programmable gate arrays). In addition to the USB connectivity, compatibility with wireless modem technology to enable communication with the central processing system (central processor/server, Figure 5.4) was essential. Unfortunately, we were unable to find a suitable platform in which a significant (i.e. useful) portion of the data acquisition and signal processing software tasks could be efficiently realized in the programmable gate arrays of these products. After 3 months of intensive testing during the last stages of this phase of the project, we abandoned further efforts. It is our opinion that with more resources and fewer constraints as far as hardware to be employed this goal could be realized if necessary as the total system of installations grows.

Chapter 7

System Deployment and Field Testing

Extensive effort was expended to prepare for field testing at the Cloquet Research facility. All aspects of the installation were completed including the communications and data acquisition hardware. Prototype sensors were evaluated on the bench top by the software discussed earlier, with this remote location sending data acquired at the Cloquet facility via wireless modem to a central processing facility located in the Chemistry Department on the University campus in Duluth. The MnDOT had promised to assist in the installation of a sensor on the concrete pad corresponding to the off ramp of this former weigh station, but was unable to provide the promised support in October of 2011. As a consequence, remote testing on an outdoor platform subject to plowing and deicing could not be completed.

References

- 1 D. Heider and A. Dominauskas, (2004) Composite Tech Brief, University of Delaware, Newark, DE (www.ccm.udel.edu).
- 2 C.-P. Lin, (2003) Frequency domain versus travel time analyses of TDR waveforms for soil moisture measurements *Soil Sci. Soc. Am.*, 67, 720.
- 3 D.A. Robinson, S.B. Jones, J.M. Wraith, D. Or and S.P. Friedman (2003) A Review of Advances in Dielectric and Electrical Conductivity Measurement in Soils Using Time Domain Reflectometry, *Vadose Zone J.*, 2, 444.
- 4 M.S. Seyfried and M.D. Murdock (1996) Calibration of time domain reflectometry for measurement of liquid water in frozen soils, *Soil Sci.*, 161, 87.
- 5 N.E. Yankielun, C.C. Ryerson and S.L. Jones (2002) Wide-Area Ice Detection Using Time Domain Reflectometry, US Army Corps of Engineers Tech. Rpt. ERDC/CRREL TR-02-15.
- 6 S. Mashimo, N. Miura and T. Umehara (1992) The structure of water determined by microwave dielectric study on water mixtures with glucose, polysaccharides, and L-ascorbic acid, *J. Chem. Phys.*, 97, 6759.
- 7 T. Sakamoto, H. Nakamura, H. Uedaira and A. Wada (1989), High-frequency dielectric relaxation of water bound to hydrophilic silica gels, *J. Phys. Chem.*, 93, 357.
- 8 John F. Evans (2009) Detection of Water and Ice on Bridge Structures by AC Impedance and Dielectric Relaxation Spectroscopy Phase I,; (2013) Detection of Water and Ice on Bridge Structures by AC Impedance and Dielectric Relaxation Spectroscopy Phase II, Center for Transportation Studies, University of Minnesota, 200 Transportation and Safety Building, 511 Washington Ave. S.E., Minneapolis, MN 55455.
- 9 John F. Evans (2013) Detection of Water and Ice on Bridge Structures by AC Impedance and Dielectric Relaxation Spectroscopy Phase II, Chapter 8, Center for Transportation Studies, University of Minnesota, 200 Transportation and Safety Building, 511 Washington Ave. S.E., Minneapolis, MN.
- 10 Instruction Manual, IRS Lufft Intelligent Road Surface Sensor, (2009), Campbell Scientific, Inc., 815 West 1800 North, Logan UT 84321.
- 11 R. N. Bracewell (2000) The Fourier Transform and Its Applications, 3rd Ed., McGraw-Hill, Boston.
- 12 S. Mallat (1999) A Wavelet Tour of Signal Processing, 2nd Ed., Academic Press, San Diego, CA.
- 13 S. Qian (2001) Introduction to Time-Frequency and Wavelet Transforms, Prentice Hall PTR, Upper Saddle River, New Jersey.
- 14 I. Daubechies (1992) Ten Lectures on Wavelets, *IEE Trans. Signal Proc.*
- 15 A. N. Akansu, W. A. Serdijn and I. W.M Selesnick (2010) Emerging Applications of Wavelets: A Review, *Phys. Comm.* 3, 1.
- 16 G. Strang, (1993) Wavelet Transforms vs Fourier Transforms, *Bull. Am. Math. Soc.*, 28, 288.